Solar Chimney Power Plants - Dimension Matching for Optimum Performance

P. J. Cottam[a], P. Duffour[a], P. Lindstrand[b], P. Fromme[c,*]

[a]*Centre for Urban Sustainability & Resilience, Department of Civil, Environmental & Geomatic Engineering, UCL, London, WC1E 6BT, UK*
[b]*Lindstrand Technologies Ltd, Oswestry, SY10 8GA, UK*
[c]*Department of Mechanical Engineering, UCL, WC1E 6BT, UK*
**contact author: p.fromme@ucl.ac.uk*

Abstract

Solar chimney power plants are very large structures with the potential to generate significant amounts of electricity. Plant dimensions such as the collector diameter and chimney height and radius are important in determining system performance. The objective of this study is to identify the key parameters that drive performance. Performance was assessed in terms of power output and power output per cost. Using a detailed thermodynamic model, the plant power output was predicted for a wide range of design and operational parameters. It was found that the optimum pressure drop ratio depends on the collector and chimney radius, but not on chimney height, ambient temperature or insolation. The dimensions of the main components must be well matched to achieve best performance. Chimney radii of up to 200 m are essential to achieve maximum power generation up to 900 MW. Optimum power output exists for variation of the collector and chimney radius. However, increasing the chimney height always results in increased power generation. The physical phenomena underpinning high-performing configurations were highlighted. Power and efficiency increase with increased plant dimensions, but technological limits exist for the chimney height. A simple but robust cost model was introduced to identify optimum configurations in terms of power output per cost. Different relative costs between collector and chimney the optimum dimensions were selected. It was concluded that several smaller plants with collector radius about 3000 m are advantageous over one larger plant. Taller chimneys are economically beneficial until the specific chimney costs increase more than quadratically with height.

Keywords
Solar updraft power plant, Solar thermal chimney, Thermodynamic model, Cost model

Nomenclature

Chimney Parameters	
R_{ch}	Chimney radius
H_{ch}	Chimney height
Δp_f	Pressure drop due to friction in the chimney
P	Power generated
Collectors Parameters	
R_c	Collector radius
h_{ci}	Collector inlet height
h_{co}	Collector outlet height
h_c	Collector height at distance *r* from inlet
α_c	Canopy absorptivity
τ_c	Canopy transmissivity
A_c	Collector annular section plan area
f_d	Darcy Friction Factor
Turbine Parameters	
x	Turbine pressure drop ratio
η_t	Turbine efficiency
Δp_t	Pressure drop available to the turbine
Ground Properties	
α_g	Ground absorptivity
T_g	Ground surface temperature
T_u	Constant ground temperature at $-5m$ underground
Working fluid Properties	
c_p	Air specific heat capacity
$\dot{m}$	Mass flow rate
ρ	Fluid density
v	Fluid velocity
p	Fluid pressure
τ	Friction shear stress
T or T_f	Temperature of the fluid
Ambient Properties	
I	Insolation
T_a	Ambient air temperature at ground level
T_s	Sky temperature
p_a	Ambient air pressure at ground level
ρ_a	Ambient air density
Heat flows	
$\dot{Q}_{12}$	Heat flow between components 1 and 2
r (index)	Reflective radiated

e (index)	Emissive radiated
c (index)	Canopy as thermal component
f (index)	Working fluid as thermal component
g (index)	Ground as a thermal component
s (index)	Sky as a thermal component
a (index)	Ambient thermal environment

1. INTRODUCTION

Solar chimney power plants (SCPP) - also called solar updraft power plants (SUPP) or Solar thermal chimneys (STC) - are large scale renewable energy plants suited for construction in regions with high insolation [1]. They typically consist of a circular solar collector to generate heated buoyant air, a tall chimney at the centre of the collector through which the buoyant air rises, and turbines and generators to extract electricity from the pressure difference as shown in Figure 1. A good overview of this technology is provided by Zhou and Xu with a focus on modelling and experimental studies [2] and Kasaeian *et al.* discussing simulations and case studies [3].

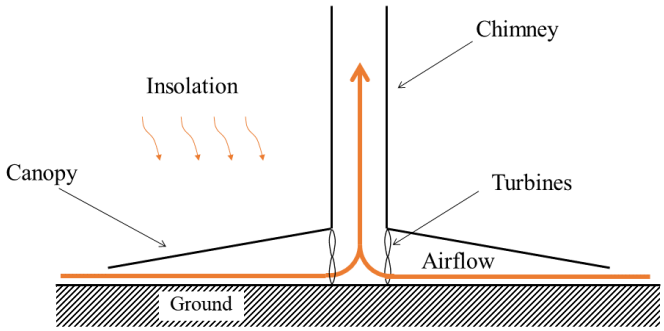

Figure 1 (color online). Schematic cross-section of a circular solar thermal chimney power plant (not to scale).

The largest experimental prototype to date, rated at 50 kW, was built and operated in Manzanares, Spain [4]. No commercial scale power plants have been constructed to date due to concerns about the economic viability and technological challenges for the construction of the tall chimneys required.

In order to predict the electricity generation and thus the expected levelized energy costs (LEC), accurate prediction of the maximum and annual power output are required, depending on the environmental conditions for planned locations and on the plant dimensions and design. Models assuming isobaric conditions within the collector have been proposed and validated with

experimental results from a small-scale physical prototype [5]. The thermodynamic cycle of the collector has been analysed [6]. More comprehensive models incorporating friction [7], ground heat loss, ambient, convective and radiative losses [8], and ambient pressure lapse rates have been developed [9, 10]. Based on a comprehensive model, using compressible gas law assumptions to describe the flow through the collector and chimney, optimum pressure drop ratios were studied for variation of the flow area parameters and solar radiation [11]. Zhou and Xu [12] developed a comprehensive model of the pressure losses throughout the system and found that the dynamic pressure drop at the chimney exit has the largest contribution.

Li *et al.* developed a comprehensive model including unsteady effects which was validated against Manzanares data [13]. A strong correlation of chimney height to efficiency and power output was predicted. Li *et al.* [14] made the case that a comprehensive model is required to accurately predict plant performance and validated their model with data from the Manzanares plant. For a plant the size of Manzanares, they investigated the effect of mass flow rate on power output and found that the turbine pressure drop ratios to achieve maximum power for different levels of insolation do not change significantly. They also found that the collector of the Manzanares plant was undersized compared to the chimney and that an increase in collector diameter would have led to an almost linear increase in power output before levelling off at significantly larger dimensions [14]. Guo *et al.* developed a 3D Computational Fluid Dynamic (CFD) model for the Manzanares plant, using solar ray-tracing, which slightly overestimated power output compared to actual measurements from Manzanares. They found that the significant effect of the collector radiation losses needs to be considered to avoid an overestimation of collector efficiency [15]. Choi *et al.* developed a comprehensive model of SCPPs and validated their results against data from Manzanares [16]. They investigated the effect of single value variation for a larger scale plant and found that water storage lowers the maximum power output but can lead to continuous electricity generation over 24 hours. Hussain and Al-Sulaiman [17] employed additional reflectors around the collector of a small prototype to increase heat generation. Simulation and experimental results predicted that this could more than double power output. Eryener *et al* [18] found that a transpired collector can improve collector efficiency significantly and demonstrated this for a small-scale prototype, having the potential to significantly reduce the area and thus cost compared to conventional glazed collectors.

The chimney is a key component of the power plant. Lupi *et al.* [1] provide an overview of solar chimney technology and looked in detail at the design of the chimney as a reinforced concrete shell similar to cooling towers. They highlighted that the wind loading falls outside current design guidelines due to the extreme height of planned chimneys. The influence of the chimney shape, slenderness, and pressure drop on flow parameters and power output were studied [19], for a cylindrical chimney with a height approximately seven times its diameter. Koonsrisuk *et al.* [20] used a simple model and scale analysis to investigate different configurations to maximize mass flow rate. For Manzanares plant dimensions, Xu and Zhu

[21] found using CFD modelling that an increased chimney outlet area (divergent, flaring chimney) leads to an increase in power output up to a maximum above which flow problems (stall, backflow, vortex) occur due to the ratio of chimney inlet and outlet areas being too large. Similarly, using CFD simulations for the Manzanares plant dimensions, Hassan *et al.* [22] found an increase in air velocity for increased slope of the collector (up to a point) and diverging chimneys, leading to expected significant increases in power generation. Novel designs for the chimney were proposed, e.g., manufactured from fabric materials and inflated with air [23] or helium [24] to achieve cost reduction. Nizetic et al [25] demonstrated from CFD simulations that the chimney could be replaced by a short diffusor to create a vortex, removing the construction complexity and cost of a tall chimney while allowing electricity generation in the MW range.

The construction of a commercial-scale SCPP is a novel and large infrastructure challenge, and the cost uncertainties are numerous and significant. Several studies have assessed potential costs of SCPP construction and a lot of disparity in calculated costs persists. Fluri *et al*. [26] studied this issue and produced a computational model of the SCPP accompanied by a comprehensive cost model including labour and finance costs. The authors compared their data to cost estimates produced by Bernades [27] and Schlaich *et al.* [28], and concluded that the costs likely exceed those calculated in these two studies, and that costs depend heavily on governmental subsidies. The capital-intensive nature of SCPP is highlighted by Li *et al.* [29], who carried out a cost study over the expected lifetime of a simulated SCPP in north-western China. The levelized electricity cost was found to initially exceed the current sales price (for the first 30-year phase), but to later reduce below the sales price, at which point the authors found that the SCPP becomes competitive with fossil fuel power generation. For a 10 MW plant in China, the annual power output was predicted using detailed meteorological data and the economic viability compared to other renewable energy ascertained [30].

An appropriate cost model can be combined with an SCPP thermodynamic model to find the cost-optimum dimensions for specific locations and proposed power plant sizes. For a small-scale prototype in Iran, experimental results and CFD simulations were evaluated to find that power output increases with chimney height and diameter [31]. Power output, costs, and overall plant efficiency were optimized by systematic variation of the plant dimensions for two prototype plants (Manzanares and Kerman, Iran) [32]. The economic feasibility for a proposed location in Nigeria was investigated using a multi-stage optimisation process employing the system efficiencies to find the best plant configuration and estimate revenues [33]. A case study was performed on a large scale SCPP in Croatia [34], calculating the expected annual electricity generation and levelized electricity costs. It was found that in the short term such a plant was not economically viable, but may have potential in the future if the life-span can be extended and costs reduced. For different plant designs and dimensions, the economic viability and pay-back periods were optimized, considering the combined plant

efficiency [35]. A proposed fabric (floating) chimney design was found to have the shortest pay-back period and reductions in plant dimensions could be achieved to obtain specific power output more economically.

Zhou *et al.* [36] studied the impact of chimney height on plant performance, identifying an optimum chimney height for fixed collector dimensions. Using a SCPP simulation with an assumed fixed collector efficiency, Dehghani and Mohammadi [37] simulated different plant configurations to optimize both cost and power generation. For the chimney diameter and collector radius cost-optimal dimensions within the study's limits were found. However in their study, power output was always optimised for chimney heights at the upper limit considered, confirming that more detailed collector efficiency and cost modelling is required to take the technological limitations associated with the chimney height into consideration. Using the comprehensive model developed previously [8], Pretorius and Kröger [38] investigated different configurations for SCPPs to achieve optimized annual power output. They found that much larger chimney diameters than considered at that time were optimal but could lead to the inflow of cold air at start-up. They proposed a systematic approach to calculate specific costs for different plant configurations, but due to computational limitations at that time, plant performance for only a limited number of dimensions could be calculated.

As outlined above, several authors have carried out parametric studies and identified optimum dimensions, both in terms of cost and best-performing dimensions of a component when all other components' dimensions are fixed. This study builds on this body of work and aims to identify the key parameters that drive performance. The thermofluid model provides new insights into why these best-performing dimensions exist, particularly for large, commercial-scale plants. Collector efficiency changes nonlinearly with the mass flow rate depending on plant dimensions, therefore a comprehensive thermofluid model is required to accurately predict power generation. A numerical model is employed to allow reasonably fast calculation of energy generation for variation of the main plant components with the required accuracy. Section 2 gives an overview of the model employed to predict energy generation, including a description of the heat transfer within the collector. Section 3 investigates the effects of different parameters on energy generation, including: the effect of turbine pressure drop ratio for a range of environmental conditions and plant dimensions; the effect of flow properties; the influence of plant dimensions on energy generation. Section 4 presents and discusses the optimization of the main plant component dimensions using a simple cost model based on collector to chimney relative costs. Section 5 concludes the manuscript.

2. MATHEMATICAL MODELLING

This study is based on a detailed steady-state model capable of simulating large-scale solar thermal chimney power plants, in a range of environmental conditions. The model simulates

the collector, chimney and turbine set separately, iterating between these components until their output and input mass-flow rates and temperatures converge to a stable steady-state solution. The model was first presented in [9] where a more detailed description can be found. The modelling approach builds on [7] and [8], and was chosen as it permits the model to operate rapidly, allowing the efficient investigation of SCPP performance across large parameter spaces, but with a sufficiently detailed thermodynamic model, especially of the collector, to accurately predict plant efficiency and thus power output.

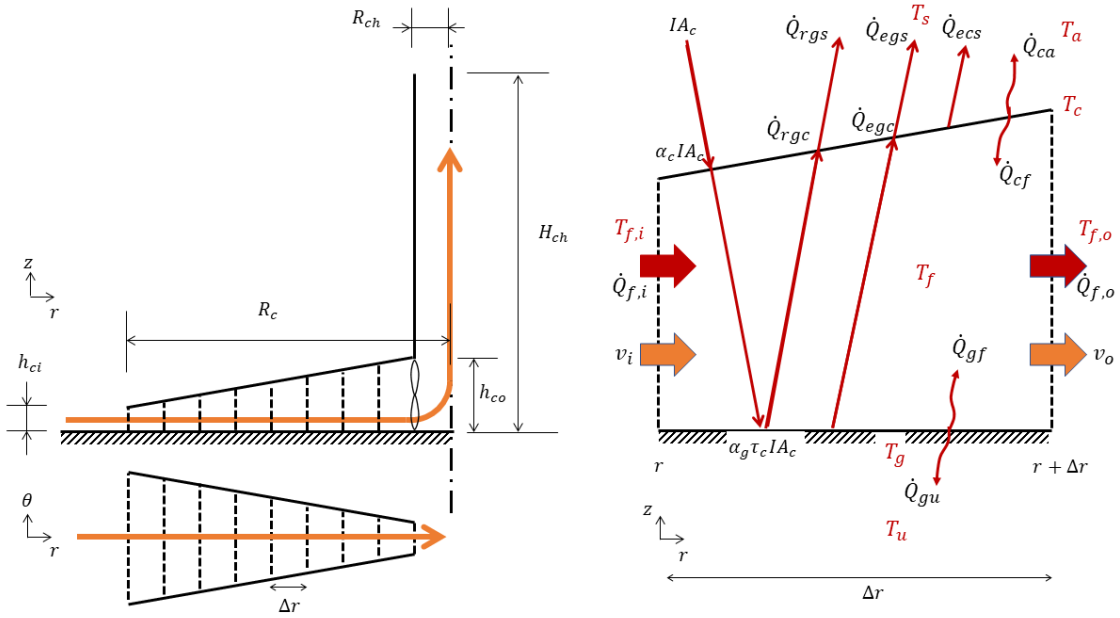

(a) (b)

Figure 2: Schematic showing: (a) plant cross-section and plan view of discretised angular sector of the collector; (b) diagram of the heat transfers within a discretised section.

The collector model assumes an incompressible, one-dimensional, axisymmetric and radial flow of the working air through a set of discretised annular sections as shown in Figure 2a. One-dimensional momentum, energy and state equations are solved at the outlet of each discretised section. The heat fluxes experienced by the working air within each section are calculated by means of a system of simultaneous equations representing the energy balance between the three thermal components considered: canopy, working air and ground. These heat fluxes are represented diagrammatically in Figure 2b. The dynamics of the air flow within the collector is described by the continuity equation (1) and the conservation of momentum equation (2):

$$\frac{1}{r}+\frac{1}{\rho}\frac{\partial \rho}{\partial r}+\frac{1}{h_c}\frac{\partial h_c}{\partial r}+\frac{1}{v}\frac{\partial v}{\partial r}=0\,, \tag{1}$$

$$\frac{\partial p}{\partial r}=-\frac{\tau}{h_c}-\rho v\frac{\partial v}{\partial r}, \tag{2}$$

where r represents the position along the collector radius measured from the outer perimeter, ρ is the fluid density, h_c is the local collector height, v the fluid velocity, p the pressures and τ the friction shear stress which was determined using $\tau=\frac{f_d \rho v^2}{8}$ where f_d is the dimensionless Darcy Friction Factor as described in [8].

The energy balance for the canopy, working fluid and ground are expressed by equations (3-5) respectively (see Figure 2b).

$$IA_c\alpha_c+\dot{Q}_{egc}+\dot{Q}_{rgc}=\dot{Q}_{ecs}+\dot{Q}_{ca}+\dot{Q}_{cf}\,, \tag{3}$$

$$\dot{m}c_p\Delta T+\frac{\dot{m}}{2}\left(v_o^2-v_i^2\right)=\dot{Q}_{cf}+\dot{Q}_{gf}, \tag{4}$$

$$IA_c\tau_c\alpha_g=\dot{Q}_{egc}+\dot{Q}_{egs}+\dot{Q}_{gf}+\dot{Q}_{gu}. \tag{5}$$

Equation (4) for the working fluid under the canopy includes kinetic and potential energy terms. The following notation conventions are used for the heat flow between components 1 and 2. $\dot{Q}_{12}$ denotes the convective energy transfer, $\dot{Q}_{e12}$ the net emitted radiation heat flow and $\dot{Q}_{r12}$ the reflected radiative heat transfer from 1 to 2. The components 1 and 2 can be any of the following: c for canopy (in this context), g for ground, f for working fluid, a for ambient air, s for sky (a theoretical horizontal plate for radiative heat loss to ambient), u for underground ground heat loss. The other notation is defined as follows: *I* is the insolation, A_c the plan collector section area, $\alpha_{c/g}$ the absorptivity of the canopy/ground, $\dot{m}$ the mass flow rate, c_p the specific heat capacity of the air, ΔT the change in temperature through the discretised section, $v_{i/o}$ the working fluid velocity at the input/output of the section, τ_c the transmissivity of the canopy.

In Equations (3)-(5), the $\dot{Q}$ terms are all of the form $hA_c\Delta T$ where h is the convective or radiative heat transfer coefficient depending on the nature of the heat flow. These coefficients were adapted from [7] and [8] as described in more detail in [9].

The thermal and mechanical evolutions of the working fluid under the canopy are coupled through equation (4) and Boussinesq approximation:

$$\frac{d\rho}{dT}=\frac{\rho}{T}\,, \tag{6}$$

valid for small changes in density which is the case here.

When written in full, theses equations constitute a linear system that can be solved for the unknown equilibrium temperatures of the canopy T_c, fluid T_f and ground T_g. The temperature of the sky T_s, surround air T_a, and underground T_u are input data to the model.

The air heated under the canopy rises through the chimney by the buoyancy pressure difference generated by the density difference between the air inside and outside the chimney. This process is modelled as adiabatic starting from a known density at ground level and includes the changes in density with altitude as expressed by:

$$\rho(h) = \rho(0)\left(1 + \frac{(\kappa-1)gh}{\kappa R T_0}\right)^{\frac{1}{\kappa-1}}, \tag{7}$$

where $\kappa = 1.235$ for ambient air and 1.4005 for working air [7], h is the height of the parcel of air considered, T_0 is the air temperature at $h = 0$ and R is the ideal gas constant.

The pressure difference eventually available to the turbine Δp_t is taken as a constant fraction x of the buoyancy pressure difference minus a pressure loss due to friction Δp_f:

$$\Delta p_t = x\left(\int_0^{H_{ch}} g(\rho_a - \rho_{ch})\mathrm{d}h - \Delta p_f\right), \tag{8}$$

where g is gravitational acceleration, $\rho_{ch/a}$ are the air densities inside/outside the chimney (resp.) at altitude h. The turbine extracts the power P from the pressure difference across it with an efficiency η_t so that:

$$P = \eta_t \frac{\dot{m}}{\rho}\Delta p_t. \tag{9}$$

The STC model outlined was implemented in Matlab. In terms of validation, it was found to satisfy continuity and conservation of momentum, and has been tested for a wide range of environmental conditions and plant dimensions. The use of the Boussinesq approximation was found to lead to a difference compared to the Ideal Gas behaviour of five orders of magnitude less than the temperature rise itself, and thus is justified. The energy balance for the complete collector was satisfied with a relative error of less than 0.1% and the energy balance for the airflow (thermal energy in minus thermal and kinetic energy out) was found to be accurate to less than 0.001%.

The comprehensive thermodynamic SCPP models presented in [7] and [8] were compared by Bernades *et al* and minor differences between the respective models were found to lead to variations in the predicted power output of up to 15%. Using the same input parameters, the power generation simulated with the model used in this paper yielded a difference of no greater than 13%, confirming that this model simulates the system accurately.

For a plant of the same reference dimensions Schlaich *et al* [28] predicted a power output of 100 MW and Fluri et al. [27] predicted a power output of 66 MW. The model presented here

predicts a power output of 74 MW for the same dimensions. In the absence of defined environmental parameters in [27] – the authors were conducting a study of power output over a year – it was assumed that insolation I = 900 W/m^2 and ambient temperature T_s = 305 K, representative of a desert environment.

Performance data from the Manzanares STC prototype was extracted from [4], along with available data on ambient temperature and material properties. For this data the simulated power output ranged from 27 kW to 35 kW, across a range of insolation values from 830 W/m^2 to 910 W/m^2 and ambient temperature from 297 K to 309 K. This was 3% to 9% less than the recorded power output from the Manzanares prototype, demonstrating that the model presented herein delivers an accurate but conservative estimate of power output.

The parametric study that follows is based on variations around reference plant of properties and environmental conditions described in Appendix A.

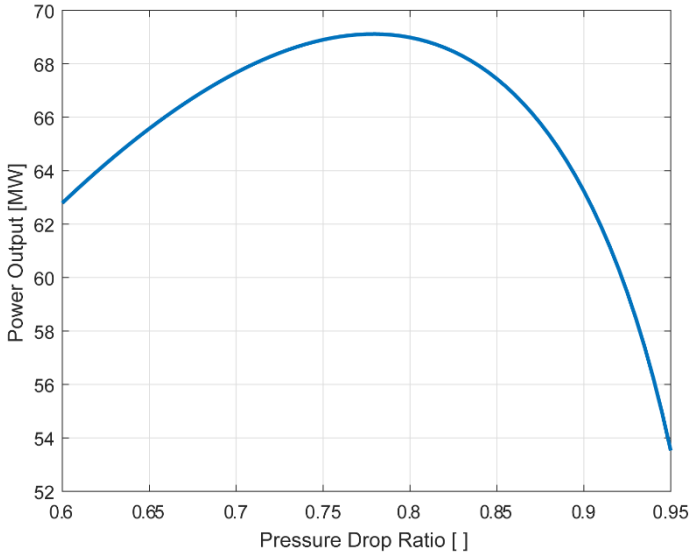

Figure 3. Power output by an SCPP under reference conditions (Appendix A) for range of turbine pressure drop ratio values x.

3. INTERACTION OF PLANT DIMENSIONS AND FLOW PROPERTIES

3.1 Optimum turbine pressure drop ratio and influence of environmental conditions

The turbine pressure drop is a key parameter in power output prediction. Its optimum value and dependence on other parameters has been studied, but remains a matter of debate [14]. Therefore, in the first part of this investigation the relationships between turbine pressure drop, power output and other parameters was studied systematically. For the plant with reference dimensions and environmental conditions, the turbine pressure drop x, was varied from 0.6 to 0.95 and the power output calculated. The results shown in Figure 3 indicate that within the

range of pressure drops investigated, the power output peaks for x around 0.8 and the power output only decreases by up to 8% for x within [0.7-0.9], in line with findings in literature [14].

Figure 4 shows surface plots of the power output in terms of the turbine pressure drop ranging from 0.6 to 0.95 for the variation of different parameters from the reference values. A white line drawn on the surface indicates the values of x for which maximum power is obtained. The insolation was also varied within 300-1100 W/m^2 but the plot looks similar to Figure 4b with almost no influence of insolation on the optimum pressure drop ratio (in line with the findings of [14]), so it is not shown here.

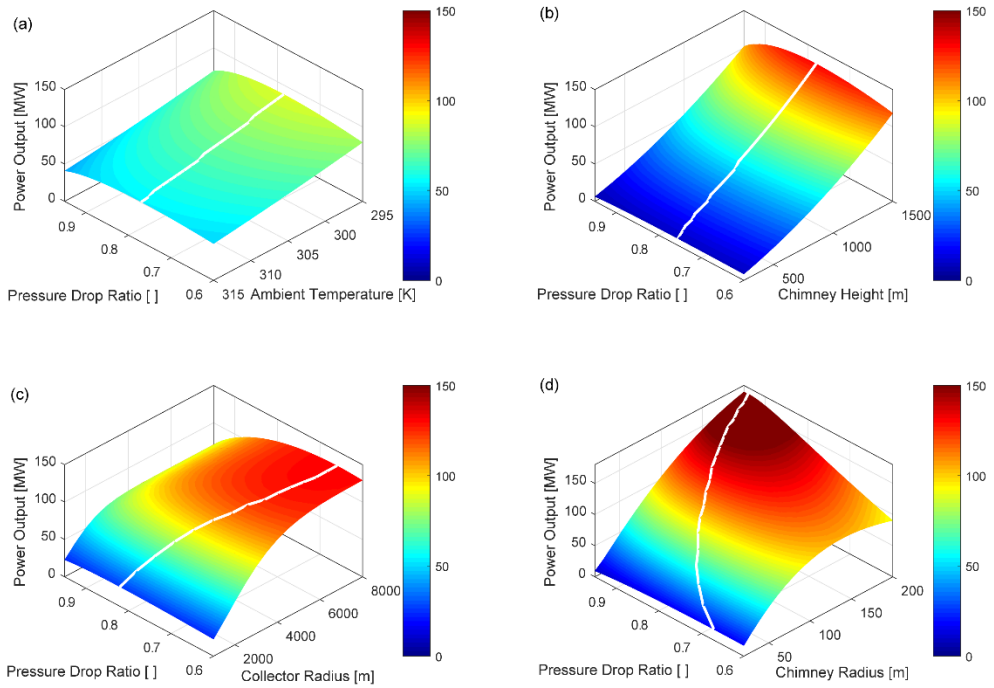

Figure 4 (color online). SCPP power output for variation of turbine pressure drop ratio and (a) ambient temperature; (b) chimney height; (c) collector radius; (d) chimney radius. All other dimensions and parameters set to reference values (Appendix A).

These plots show that for the parameter ranges considered, the maximum power output is consistently obtained for a turbine pressure drop between 0.7 and 0.9. The value of x giving maximum power changes very little when ambient temperature (Figure 4a) and chimney height (Figure 4b) are varied within wide ranges. It increases almost linearly from 0.65 to 0.85 with increasing collector radius (Figure 4c). As the collector size increases, the air temperature and thus pressure difference increases, allowing a larger proportion to be used to drive the turbine and generate electricity. For increased chimney radii (Figure 4d), increased air flow is possible, but the reference collector becomes undersized and prevents optimal flow conditions to develop, thereby restricting power output. This effect is partially compensated by reducing the

turbine pressure drop, i.e. by allowing more flow through. The surfaces are remarkably flat around the optimum, indicating that the power output is not very sensitive to the exact value of the pressure drop. Consequently, a fixed value of 0.8 was used throughout the remainder of this study.

3.2 Influence of main plant dimensions on power output

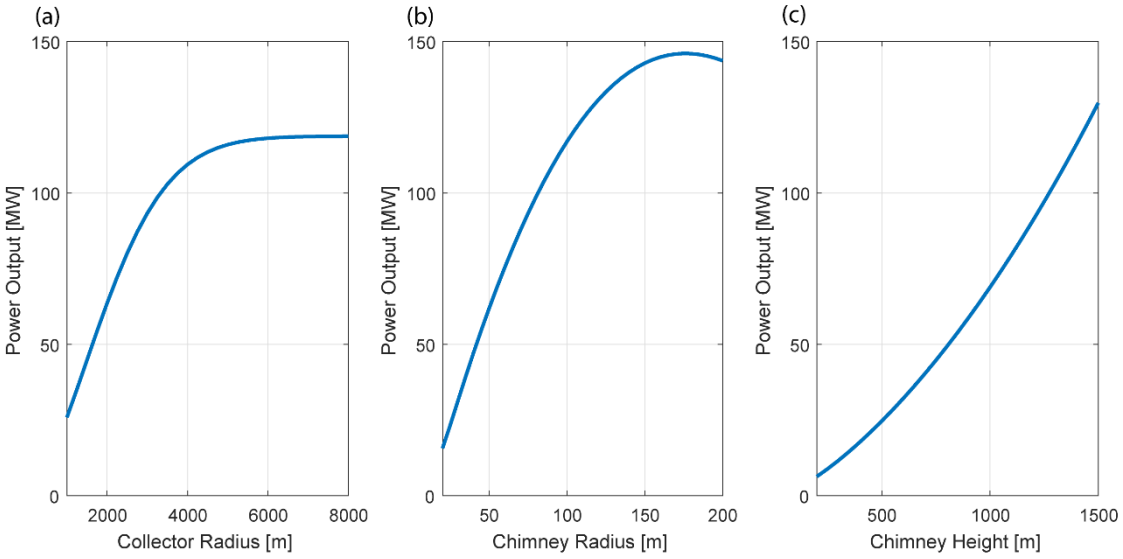

Figure 5. SCPP power output curves for varying SCPP component dimensions: (a) collector radius; (b) chimney radius; (c) chimney height. All other dimensions set to reference values (Appendix A)

In this section, the influence of overall SCPP plant dimensions on power output is investigated. In Figure 5a, the power output is seen to increase from 25MW for a collector radius of 1000m to 115MW for a collector radius of 8000m. This increase is almost linear up to about 3000m radius, as increased collector size leads to increased heat input. It is interesting to note that the increase is almost linear with collector radius, but not with area (which increases with the collector radius squared). The power output then plateaus towards its maximum for larger collector radii above 5000m. This shows that when the other dimensions are fixed, increasing the collector size beyond a certain size brings diminishing returns. Figure 5b shows similarly that the power output increases almost linearly from 20MW for low chimney radii (20m), as an increased chimney cross-section allows for increased air flow. It reaches a maximum of 145MW at a 165m radius and then marginally decreases for chimney radii up to 200 m. This maximum is relatively flat so that a power in excess of 140 MW would be obtained for any chimney radius within the 120m-200m range. **C**himney structures with very large flow area are susceptible to a phenomenon called cold air inflow, which also afflicts cooling towers. Pretorius and Kroger [8] assessed a chimney's susceptibility to cold air inflow using the densimetric Froude Number Fr_D, which represents the ratio of inertial to gravitational forces acting on the working air at the chimney outlet. They found that for the range of SCPP

configurations around the optimum, cold air inflow would not be an issue. Following their methodology, we arrived at the same conclusion in this study.

The power output increases significantly with chimney height (Figure 5c). The model predicts a power output of 8 MW for a 200m-high chimney, up to 130 MW for a chimney 1500m high. Within the range considered, the predicted power output (all other reference dimensions fixed) is well approximated by a quadratic variation with chimney height as can be found from fitting the curve in Figure 5c. Therefore, in terms of power output alone, the higher the chimney, the better the plant performance. This is in line with findings by Dehghani and Mohammadi [37], who found cost-optimal dimensions for the chimney diameter and collector radius, while power output optimised for the upper limit of the chimney heights considered.

3.3 Interaction between flow properties, overall dimensions and power output

To better understand how the dimensions of the main components interact with each other, it is instructive to look at how the air flow properties change under the collector for plants of various collector sizes. Figure 6 shows how the temperatures of the canopy, working air and ground vary along the collector radius for SCPP plants with three different collector radii: 1000m, 2500m and 4000m. The chimney is centred at zero collector radial path (the horizontal axis of this graph), so the air enters right and moves leftward in the graph. It can be seen that the ground temperature is always above the canopy temperature. For all collector sizes, the fluid temperature starts at T_∞ = 305 K at the collector inlet (ambient) and initially increases as it travels towards the chimney. For smaller collector sizes (1000m radius) the air temperature does not reach the canopy temperature. This is because the heat input over the distance travelled by the air is not sufficient for it to store enough thermal energy. For a collector radius of 2500 m a significant increase in air temperature over the complete collector radial path can be observed so that the air temperature reaches the canopy temperature close to the chimney. By contrast, for large collectors, for example 4000m, the air reaches a temperature between that of the ground and the canopy at around 2800 m radial path. It then increases rather slowly as the air moves further towards the chimney. Therefore, for a given chimney radius and height, the collector must be large enough for the airflow to reach a temperature between the other two components, but a much larger collector does not bring much added benefit as the three thermal components reach an equilibrium. The reduction in temperatures close to the chimney is due to rapid increases in air velocity as the flow becomes constricted.

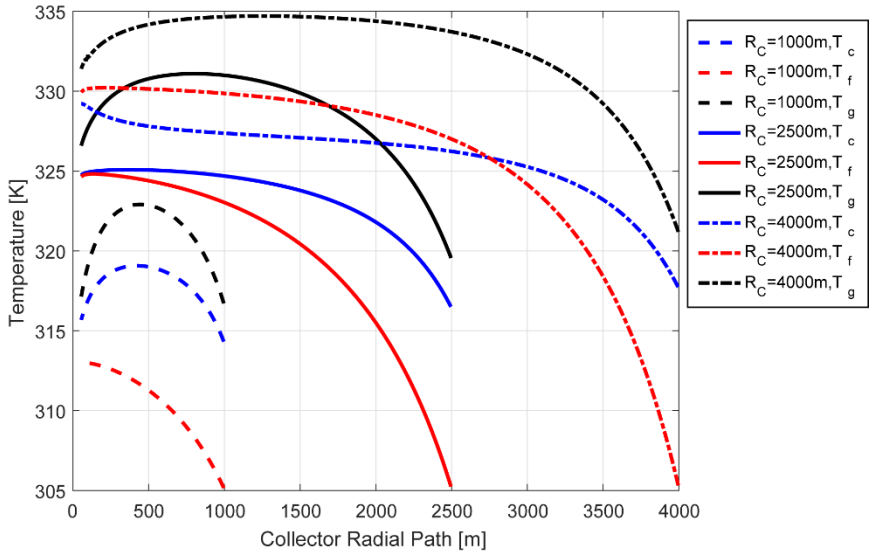

Figure 6 (color online). Temperature along collector radial path for air (red), ground (black) and canopy (blue); SCPPs with three different collector radii: 1000m (dashed), 2500m (solid) and 4000m (dash-dotted).

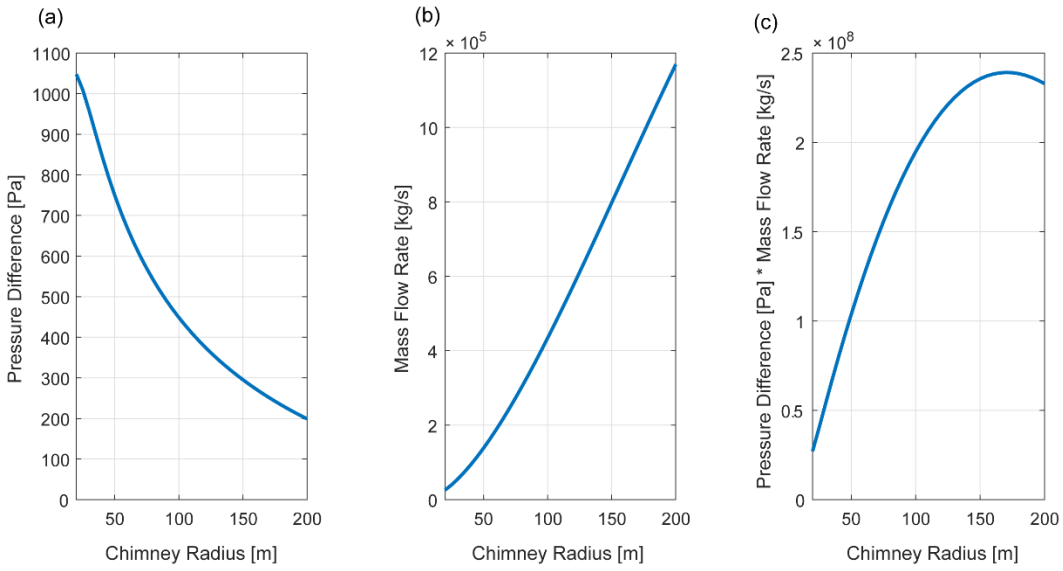

Figure 7. (color online) Chimney inlet pressure potential (a) and system mass flow rate (b) for varying collector radius. The product (c) is proportional to the power output. R_c = 3000 m; H_{ch} = 1000 m.

Considering a series of SCPPs with a fixed chimney height (H_{ch} = 1000 m), a fixed collector radius (R_c = 3000 m), and chimney radii varying between 20m and 200m, Figure 7a shows the pressure difference generated by the SCPP at the chimney inlet, Figure 7b shows the mass flow rate generated for different chimney radii. The pressure difference generated by the SCPP falls and the mass flow rate increases as the chimney radius increases. The SCPP power output is proportional to the product of mass flow rate and chimney inlet pressure difference (see Eq. 9), and Figure 7c shows how this product combines reducing pressure difference with increasing mass flow rate to reach a peak for a relatively large

chimney radius (165m) before falling again. This explains the observed maximum in power output obtained when the chimney radius is varied (Figure 5b) and indicates that for the other dimensions fixed an optimum chimney radius can be found to maximize power output. The same behaviour of decreasing pressure difference and increasing mass flow rate was observed for increasing chimney heights by Zhou et al [36].

3.4 Importance of dimension matching

Figure 8 shows plots of power output for plants with collector radii varying from 2000m to 8000m and chimney radii ranging from 20m to 200m. Typically the maximum height of the chimney would be determined by construction feasibility and costs, therefore the other dimensions are investigated for two different fixed chimney heights: H_{ch} = 500m (Figure 8a), H_{ch}=1000m (Figure 8b).

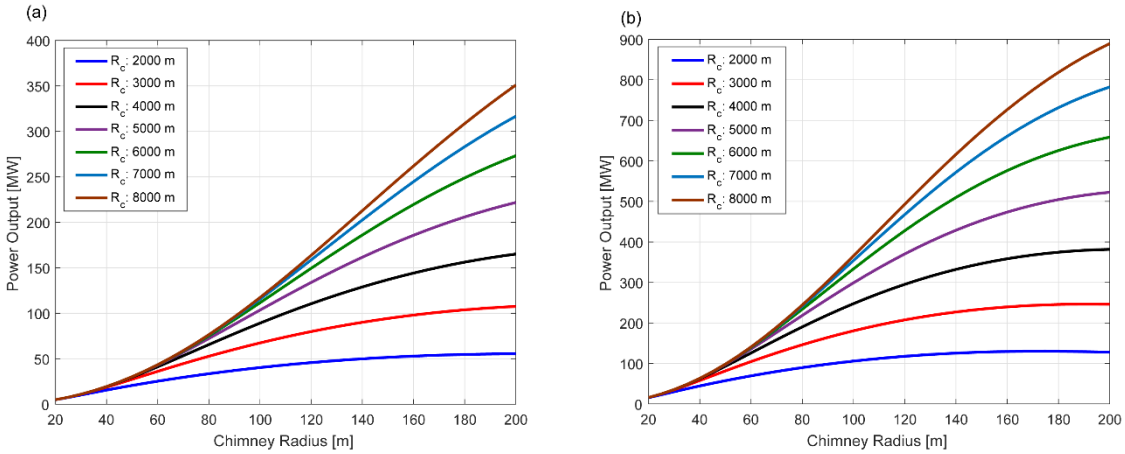

Figure 8. (color online) SCPP power output for varying combinations of chimney radius and collector radius; a) H_{ch} = 500 m; b) H_{ch} = 1000 m.

As expected, the power output increases with increasing collector and chimney radius for both chimney heights. However, the height of the chimney significantly affects the maximum power reached. For H_{ch} = 500m, a plant with the largest collector and chimney radius considered would produce about 350MW, whereas a plant with a 1000m tall chimney and the same collector and chimney radius is predicted to generate up to 900MW. Two performance-limiting mechanisms are apparent in Figure 8. The first is visible as the rate of increase of the power output decreases for increasing chimney radius for any fixed collector radius. For the smaller collector sizes considered, the power output plateaus and increased chimney radius does not result in increased power output. This upper limit does however increase with collector radius and chimney height. Secondly, for fixed chimney radius the increase in power output with increased collector radius decreases, e.g. for a chimney with 1000m height and 100m radius, only a small increase in power output occurs beyond a collector radius of 6000m. This is due to the thermal equilibrium reached between collector components which causes the power output to increase at a reduced rate despite increases in collector size, as discussed in section 3.3.

Only if both the collector and chimney radius are increased, does the power output increase significantly. From these simulations, it is clear that plants of larger dimensions will always lead to

increased power output, even if this increase tends to plateau. Therefore, optimising the energy generation by varying overall plant dimensions will lead to an optimum at the top of the parameter range considered. Costs must be considered to identify a true optimum.

4. PLANT OPTIMISATION INCLUDING COST

4.1 Cost modelling assumptions

Cost and investment models for SCPPs of varying degrees of complexity and at different locations have been proposed in the literature (see section 1, e.g. [29, 35]). Costs and investment incentives (e.g. carbon credits, tax rates [30]) can vary considerably between locations and can change rapidly over time. This makes comparisons and robust financial analysis difficult. Annual power generation depends on the cumulative electricity generation for the varying meteorological conditions over the year for a given plant size and location [34], a good indication of the economically most effective plant dimensions can be obtained by comparing the maximum power output (for a fixed insolation) to the construction costs. Available relatively detailed construction cost models have been based on advanced plant designs (e.g. [26]) and assumptions regarding many external factors which are difficult to verify in early stages of the technological development. Therefore, a simplified approach was adopted here, based on a nominal unit cost per surface area for the collector and non-dimensional costs of the chimney and turbine set relative to the collector unit cost. This provides a robust comparison of capital expenditure on which more detailed site and time specific financial forecasting can be based.

Assuming a constant unit cost per square metre of collector surface can be justified by the large scale and relative simplicity of construction involved. Previous, more detailed investigations of the collector canopy shape have demonstrated that most of the collector area can be kept flat with only an increase in height for a relatively small area around the chimney, with no significant drop in power output [9]. The chimney construction costs and how they scale with dimensions is much more difficult to determine. Detailed design for reinforced concrete chimneys with a height of 1000m and diameter of 150m has been proposed [1]. However, significant variations between different sources can be found, e.g. Pretorius and Kröger [38] assume an average wall thickness of 1m, while the design by Lupi *et al.* [1] has an average wall thickness of 0.345m. Within the range of large chimney diameters considered, the simplest assumption adopted here in the first instance is that the construction method does not change with chimney radius, so that cost increases linearly with circumference. Other assumptions regarding the dependence of chimney cost with height will be explored in the following section.

The specific costs for chimney (per square meter of surface area) and the turbines (per Watt of peak power generated) were calibrated using the relative costs of the collector (per surface area), chimney and turbine components calculated by Fluri *et al*. in their comprehensive assessment of SCPP costs for a 1000m tall chimney [26] (Configuration II, based on [28]). These are given it Table 2.

Table 2. Non-dimensional specific cost for SCPP cost constraints in optimisation process. Normalised at collector cost = 1 unit per m^2, based on Fluri *et al* [26].

Component	**Non-dimensional specific cost**
Collector	1 per m^2 of collector area
Chimney	12.24 per m^2 of chimney inner surface area.
Turbine	0.012 per W of peak power generated.

4.2 Cost performance analysis for fixed chimney height and Collector/Chimney cost ratios

Using the above assumptions, one can calculate the power output per non-dimensional cost unit for each configuration. Figure 9 shows how the power output per unit cost varies against the same parameter space as Figure 8. The highest power output per unit cost is achieved for a 1000m tall chimney, a chimney radius of 165m, a collector radius of 3250m, and a power output of 272 MW. The power output per non-dimensionalised cost unit is 5.5 W/unit.

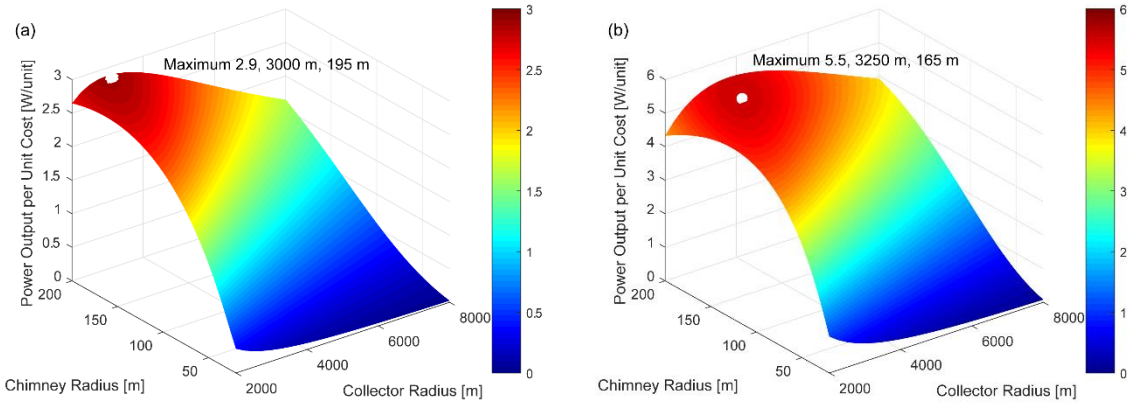

Figure 9 (color online). Power output per unit cost for SCPPs with varying collector and chimney radii; a) 500 m; b) 1000 m chimney height; maximum point indicated.

Figure 9 shows that exceptionally large collectors (with a radius greater than 5000m) are not economically optimal unless the chimney flow area is commensurably increased. This can be understood from Figure 5a, which showed an initial linear increase in power plateauing off with collector radius, in line with the reduced collector efficiency for larger collector radii found by [32]. As collector costs increase quadratically with radius (area), the power output per collector cost decreases. As the chimney and power conversion costs contribute a significant percentage to overall costs, an optimum collector radius can be found. Increasing chimney radii lead to an increase in power output and a linear increase of chimney costs. Therefore, in general large chimney radii are beneficial, but as seen in Figure 7c, a maximum in the power output can be obtained. Increasing the chimney height yields a significant improvement in performance for all configurations except those with a combination of exceptionally large collector area and small chimney flow area. With the linear increase in chimney cost with height assumed here (constant cost per chimney surface area), the power output per unit cost will always increase with chimney height, as the power output relates quadratically to chimney height (Figure 5c). This correlates with the findings by Dehghani and Mohammadi [37] and Nizetic et al [34], who found that the increase in chimney efficiency with height leads to an increase of the overall low plant efficiency.

4.3 Sensitivity to cost ratios and chimney cost variation with height

To investigate the robustness of the previous results, a sensitivity analysis was carried. First the relative cost of the chimney to collector was varied in a range of 6.12 to 24.48 per m^2 (half and double the estimates by Fluri [26]) for chimney heights of 500m, 750m, and 1000m. Secondly, variation of chimney specific cost with height was considered. The cost increase with increased chimney height is

likely more than linear (surface area), as taller chimneys will be exposed to increased self-weight and wind loading leading to increased bending loads. Pretorius and Kröger [38], and Li *et al.* [29] assumed a quadratic increase in cost with height due to the average wall thickness increasing with height. It might be argued that due to limitations of current construction technology for extremely tall structures and wind loading leading to increased bending moments, that cost increases even more with height, and a cubic increase of costs with chimney height was considered as well. Therefore, in addition to the linear cost function with height previously investigated, a quadratic, and a cubic increase of chimney specific costs with chimney height were considered. These chimney cost functions were normalized such that they all have the same cost for a 1000m tall chimney.

Results from varying the specific costs of the chimney and turbine relative to that of the collector are shown in Table 3. For all chimney heights it was found that for relatively lower specific costs of the chimney, the optimum dimensions tended towards smaller collector and chimney radii. For higher relative costs of the chimney, a larger collector provides more heat to the air and the increased costs for increased chimney radii are balanced by the higher generated power. This results in lower power output per cost unit.

Table 3. Sensitivity analysis of optimal dimensions for different ratios of component unit costs and chimney heights. All costs are given relative to the collector, which has a specific cost of 1 unit/m^2 of collector area.

Relative chimney cost (units)	**Relative turbine cost (units)**	H_{ch} **(m)**	**Optimum** R_{ch} **(m)**	**Optimum** R_c **(m)**	**Specific power output (W/unit)**
6.12	0.006	1000	160	2500	6.8
12.24	0.012	1000	165	3250	5.5
18.36	0.036	1000	180	4000	4.8
24.48	0.024	1000	180	4250	4.3
6.12	0.006	750	175	2500	5.1
12.24	0.012	750	185	3250	4.2
18.36	0.036	750	190	3750	3.7
24.48	0.024	750	195	4250	3.4
6.12	0.006	500	190	2250	3.4
12.24	0.012	500	195	3000	2.9
18.36	0.036	500	195	3250	2.6
24.48	0.024	500	200	3500	2.4

With the assumption of chimney cost varying linearly with height, it was found that the optimum is always at the highest chimney, as power output increases quadratically with chimney height. As the previous optima were obtained for a collector radius around 3250m, a cost analysis was carried out with a fixed collector at that value while varying the chimney height and radius. Figure 10a shows that for a quadratic increase of specific costs with height the optimum power output per unit cost is still obtained for the tallest chimney considered. Power output increases quadratically with chimney height, and as

collector costs make up a significant part of the overall costs the ratio improves. Interestingly, the optimum chimney radius decreases with chimney height as the taller chimney provides increased updraft and the slight improvement in power output obtained with wider chimneys is negated by the increased costs. This in line with the findings by Pretorius and Kroger [38], who found that plants with the greatest chimney height were considerably more cost effective, but noted that the increase in specific costs with chimney dimensions were underestimated in their cost model. Considering a cubic variation of specific chimney costs with height, the increase in power output does not keep up with costs and an optimum value is obtained, at a specific ratio of 5.9 W/cost unit at a chimney height of 1450m and chimney radius of 130m for the parameters considered here. Again, a decrease in optimum chimney radius with chimney height is observed. It must be noted that the maximum in Figure 10b is rather flat, i.e., for chimney heights between 1000 and 2000m the power output to cost ratio changes only by about 10% and the exact optimum depends on the assumed relative costs.

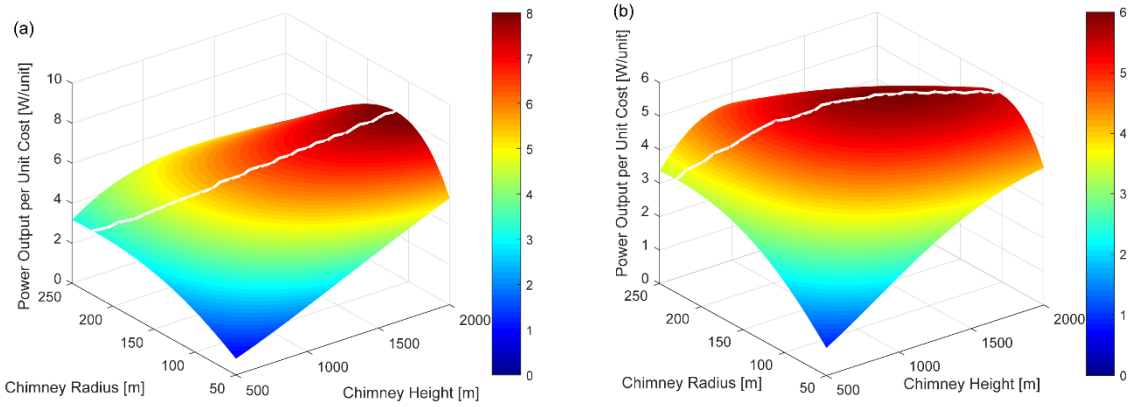

Figure 10. Power output per unit cost for SCPPs with varying chimney height and radius; 3250m collector radius; a) quadratic; b) cubic increase of specific cost with chimney height.

Therefore, when cost is taken into consideration, the best performing SCPP configurations are not those with the largest chimney diameter, or the largest collector. This suggests that multiple smaller (but still very large) SCPPs may be better suited to achieve the lowest cost per unit of energy produced. However, tall chimneys are shown to be essential for achieving the greatest possible power output per unit cost. For such a tall structure, the assumptions regarding the specific costs remains highly uncertain, as the risks and technical challenges increase with increasing chimney height.

5. CONCLUSIONS

This aim of this paper was to investigate systematically the key performance drivers for Solar Chimney Power Plants. This was achieved using a comprehensive thermofluidic numerical model and a simple but robust cost model. The detailed output from the thermofluid model provided novel insight into the physical processes underpinning power output. The coupling with the simple cost model sheds new light on the interaction between plant thermodynamic performance and capital expenditure.

It was shown that:

- For given plant dimensions, optimum power output is not sensitive to the turbine pressure drop for a wide range of environmental conditions, in line with previous findings in literature.
- Electricity generation initially increases linearly with collector radius and chimney radius, before plateauing off or reaching a maximum.
- Power output increases quadratically with chimney height confirming the need to design plants with tall chimneys.
- For a given chimney height, the collector size must be carefully matched with the chimney radius.
- The collector radius must be large enough for the air temperature to reach equilibrium with the canopy and ground. However, increasing the radius beyond this point brings no additional benefit.
- Narrow chimneys constrict the flow and consequently limit power output. Chimney radii of up to 200 m are necessary to reach power output of 900 MW.
- Based on thermodynamic modelling alone, larger plants will always lead to increased power output. Therefore, any power optimisation scheme that does not consider cost will return optimum plant sizes at the top of the ranges considered.
- Optimisation of power output using the thermodynamic model coupled with the cost model indicated that several smaller plants with collector radius of about 3000 m may be advantageous over one larger power plant.
- The way the specific chimney cost increases with height governs the existence of power per cost optimum. If this dependence is quadratic or lower, taller chimneys will always be economically beneficial. When the dependence is cubic or higher, plant dimensions giving a true optimum in power output exist, but these are still extremely large.

More detailed conclusions are highly dependent on improved cost assessments, requiring more advanced chimney designs and further technological development.

ACKNOWLEDGEMENTS

The authors are grateful to the UK Engineering & Physical Sciences Research Council (EPSRC), UCL Centre for Urban Sustainability & Resilience [Grant EP/G037698/1], Lindstrand Technologies Ltd, the Royal Society, and the Royal Commission for the Exhibition of 1851 for their support of this research and the studentship of P. Cottam.

References

[1] F. Lupi, C. Borri, R. Harte, W.B. Kratzig, H.-J. Niemann, "Facing technological challenges of Solar Updraft Power Plants," Journal of Sound and Vibration 334, 57–84 (2015). https://doi.org/10.1016/j.jsv.2014.03.010

[2] X. Zhou, Y. Xu, "Solar updraft tower power generation," Solar Energy 128, 95-125 (2016). https://doi.org/10.1016/j.solener.2014.06.029

[3] A.B. Kasaeian, S. Molana, K. Rahmani, D. Wen, "A review on solar chimney systems," Renewable and Sustainable Energy Reviews 67, 954–987 (2017). https://doi.org/10.1016/j.rser.2016.09.081

[4] W. Haaf, K. Friedrich, G. Mayr, J. Schlaich, “Solar Chimneys Part I: Principle and Construction of the Pilot Plant in Manzanares,” International Journal of Solar Energy, 2, 3–20 (1983). https://doi.org/ 10.1080/01425918308909911
[5] X. Zhou, J. Yang, B. Xiao, G. Hou “Simulation of a pilot solar chimney thermal power generating equipment,” Renewable Energy 32, 1637–1644 (2007). https://doi.org/10.1016/j.renene.2006.07.008
[6] A.J. Gannon, T.W. von Backström, “Solar chimney cycle analysis with system loss and solar collector performance,” Journal of Solar Energy Engineering 122, 133-137 (2000). https://doi.org/10.1115/1.1314379
[7] M.A. dos S. Bernardes, A. Voß, G. Weinrebe, “Thermal and technical analyses of solar chimneys,” Solar Energy 75, 511–524 (2003). https://doi.org/10.1016/j.solener.2003.09.012
[8] J.P. Pretorius, D.G. Kröger, “Solar Chimney Power Plant Performance,” Journal of Solar Energy Engineering 128, 302–311 (2006). https://doi.org/10.1115/1.2210491
[9] P.J. Cottam, P. Duffour, P. Lindstrand, P. Fromme, “Effect of canopy profile on solar thermal chimney performance,” Solar Energy 129, 286-296 (2016). https://doi.org/10.1016/j.solener.2016.01.052
[10] W.B. Krätzig, “An integrated computer model of a solar updraft power plant,” Advances in Engineering Software 62–63, 33–38 (2013). https://doi.org/10.1016/j.advengsoft.2013.04.018
[11] X. Zhou, Y. Yu, Y. Hou, “Effect of flow area to fluid power and turbine pressure drop factor of solar chimney power plants,” Journal of Solar Energy Engineering 139, 041012 (2017). https://doi.org/10.1115/1.4036774
[12] X. Zhou, Y. Xu, “Pressure losses in solar chimney power plant,” Journal of Solar Energy Engineering 140, 024502 (2018). https://doi.org/10.1115/1.4038962
[13] J. Li, H. Guo, S. Huang, “Power generation quality analysis and geometric optimization for solar chimney power plants,” Solar Energy 139, 228–237 (2016). https://doi.org/10.1016/j.solener.2016.09.033
[14] J.-Y. Li, P.-H. Guo, Y. Wang, “Effects of collector radius and chimney height on power output of a solar chimney power plant with turbines,” Renewable Energy 47, 21-28 (2012). https://doi.org/ 10.1016/j.renene.2012.03.018
[15] P.-H. Guo, J.-Y. Li, Y. Wang, “Numerical simulations of solar chimney power plant with radiation model,” Renewable Energy 62, 24-30, (2014). https://doi.org/10.1016/j.renene.2013.06.039
[16] Y.J. Choi, D.H. Kam, Y.W. Park, Y.H. Jeong, “Development of analytical model for solar chimney power plant with and without water storage system,” Energy 112, 200-207 (2016). https://doi.org/10.1016/j.energy.2016.06.023
[17] F.M. Hussain, F.A. Al-Sulaiman, “Performance analysis of a solar chimney power plant design aided with reflectors,” Energy Conversion and Management 177, 30-42 (2018). https://doi.org/10.1016/j.enconman.2018.09.043
[18] D. Eryener, J. Hollick, H. Kuscu, “Thermal performance of a transpired solar collector updraft tower,” Energy Conversion and Management 142, 286-295 (2017). https://doi.org/10.1016/j.enconman.2017.03.052
[19] T. Ming, R. Kiesgen de Richter, F. Meng, Y. Pan, W. Liu, “Chimney shape numerical study for solar chimney power generating systems,” International Journal of Energy Research 37, 310-322 (2013). https://doi.org/10.1002/er.1910

[20] A. Koonsrisuk, S. Lorente, A. Bejan, "Constructal solar chimney configuration," International Journal of Heat and Mass Transfer 53, 327-333 (2010). https://doi.org/10.1016/j.ijheatmasstransfer.2009.09.026
[21] Y. Xu, X. Zhou, "Performance of divergent-chimney solar power plants," Solar Energy 170, 379-387 (2018). https://doi.org/10.1016/j.solener.2018.05.068
[22] A. Hassan, M. Ali, A. Waqas, "Numerical investigation on performance of solar chimney power plant by varying collector slope and chimney diverging angle," Energy 142, 411-425 (2018). https://doi.org/10.1016/j.energy.2017.10.047
[23] V. Putkaradze, P. Vorobieff, A. Mammoli, N. Fathi, "Inflatable free-standing flexible solar towers," Solar Energy 98, 85–98 (2013). https://doi.org/10.1016/j.solener.2013.07.010
[24] C.D. Papageorgiou, M. Psalidas, S. Sotiriou, "Floating solar chimney technology scale analysis," Proceedings of the IASTED International Conference on Power and Energy Systems, EuroPES 2011, 55-59 (2011). https://doi.org/ 10.2316/P.2011.714-052
[25] S. Nizetic, Z. Penga, M. Arici, "Contribution to the research of an alternative energy concept for carbon free electricity production: Concept of solar power plant with short diffuser," Energy Conversion and Management 148, 533-553 (2017). https://doi.org/10.1016/j.enconman.2017.05.062
[26] T.P Fluri, J.P. Pretorius, C.V. Dyk, T.W. von Backström, D.G. Kröger, G.P.A.G. van. Zijl, "Cost analysis of solar chimney power plants," Solar Energy 83, 246–256 (2009). https://doi.org/10.1016/j.solener.2008.07.020
[27] M.A. dos S. Bernardes, "Technische, ökonomische und ökologische Analyse von Aufwind-kraftwerken," PhD Thesis, Universität Stuttgart (2004).
[28] J. Schlaich, R. Bergermann, W. Schiel, G. Weinrebe, "Sustainable Electricity Generation with Solar Updraft Towers," Structural Engineering International 14, 225–229 (2004). https://doi.org/10.2749/101686604777963883
[29] W. Li, P. Wei, X. Zhou, "A cost-benefit analysis of power generation from commercial reinforced concrete solar chimney power plant," Energy Conversion and Management 79, 104–113 (2014). https://doi.org/10.1016/j.enconman.2013.11.046
[30] P. Guo, Y. Zhai, X. Xu, J. Li, "Assessment of levelized cost of electricity for a 10-MW solar chimney power plant in Yinchuan China," Energy Conversion and Management 152, 176-185 (2017). https://doi.org/10.1016/j.enconman.2017.09.055
[31] K.M. Shirvan, S. Mirzakhanlari, M. Mamourian, N. Abu-Hamdeh, "Numerical investigation and sensitivity analysis of effective parameters to obtain potential maximum power output: A case study on Zanjan prototype solar chimney power plant," Energy Conversion and Management 136, 350–360 (2017). https://doi.org/10.1016/j.enconman.2016.12.081
[32] E. Gholamalizadeh, M.-H. Kim, "Thermo-economic triple-objective optimization of a solar chimney power plant using genetic algorithms," Energy 70, 204-211 (2014). https://doi.org/10.1016/j.energy.2014.03.115
[33] C.O. Okoye, O. Solyalı, O. Taylan, "A new economic feasibility approach for solar chimney power plant design," Energy Conversion and Management 126, 1013–1027 (2016). https://doi.org/10.1016/j.enconman.2016.08.080
[34] S. Nizetic, N. Ninic, B. Klarin, "Analysis and feasibility of implementing solar chimney power plants in the Mediterranean region," Energy 33, 1680– 1690 (2008). https://doi.org/10.1016/j.energy.2008.05.012

[35] B. Ali, “Techno-economic optimization for the design of solar chimney power plants,” Energy Conversion and Management 138, 461–473 (2017). https://doi.org/10.1016/j.enconman.2017.02.023
[36] X. Zhou, J. Yang, B. Xiao, G. Hou, F. Xing, “Analysis of chimney height for solar chimney power plant,” Applied Thermal Engineering 29, 178-185 (2009). https://doi.org/10.1016/j.applthermaleng.2008.02.014
[37] S. Dehghani, A.H. Mohammadi, “Optimum dimension of geometric parameters of solar chimney power plants – A multi-objective optimization approach, Solar Energy 105, 603–612 (2014). https://doi.org/10.1016/j.solener.2014.04.006
[38] J.P. Pretorius, D.G. Kröger, “Thermoeconomic optimization of a solar chimney power plant,” Journal of Solar Energy Engineering 130, 021015 (2008). https://doi.org/10.1115/1.2840571

Appendix A

Table A: Input parameter reference values.

Parameter	Reference value
Collector	
R_c – Collector radius	2150 m
h_{ci} – Canopy inlet height	4 m
h_{co} – Canopy outlet height	20 m
α_c – Canopy absorptivity	0.30
τ_c – Canopy transmissivity	0.70
Chimney	
R_{ch} – Chimney radius	55 m
H_{ch} – Chimney height	1000 m
Turbine	
x – Turbine pressure drop ratio	0.81
η_t – Turbine efficiency	0.75
Ground	
ϵ_g – Ground emissivity	0.90
α_g – Ground absorptivity	0.90
ρ_{rg} – Ground reflexivity	0.10
ρ_g – Ground density	2160 kg/m^3
c_{pg} – Ground specific heat capacity	710 Jkg^{-1}K^{-1}
k_g – Ground conductivity	1.83 Wm^{-1}K^{-1}
z_b – Ground depth at which $dT/dz = 0$	5 m
T_u – Ground constant temperature at z_b	283 K
Air	
T_a – Ambient air temperature at ground level	305 K
p_a – Ambient air pressure at ground level	101325 Pa
c_p – Air specific heat capacity	1008.5 Jkg^{-1}K^{-1}
RH – Air relative humidity	0.2
I – Insolation	900 Wm^{-2}